Solitons in quadratic nonlinear photonic crystals

J. F. Corney and Ole Bang
Informatics and Mathematical Modelling, Technical University of Denmark, Building 321, 2800 Kongens Lyngby, Denmark
(Received 12 January 2001; published 21 September 2001)

We study solitons in one-dimensional quadratic nonlinear photonic crystals with modulation of both the linear and nonlinear susceptibilities. We derive averaged equations that include induced cubic nonlinearities, which can be *defocusing*, and we numerically find previously unknown soliton families. Because of these induced cubic terms, solitons still exist even when the *effective quadratic nonlinearity vanishes* and conventional theory predicts that there can be no soliton. We demonstrate that both bright and dark forms of these solitons can propagate stably.

DOI: 10.1103/PhysRevE.64.047601 PACS number(s): 42.65.Tg, 05.45.Yv, 42.65.Jx, 42.65.Ky

The physics and applications of photonic band-gap (PBG) materials, or *photonic crystals*, have been active topics of research for more than a decade. The theory of linear photonic crystals is now well understood, and many of their fundamental properties and technical applications have been characterized [1]. The next important step in the application of photonic crystals is to create tunable PBGs. Tunability is possible in linear photonic crystals through, e.g., the temperature dependence of the refractive index [2] or the electro-optic effect [3]. Ultrafast dynamical tunability of the PBG can be accomplished using nonlinearity, as was first demonstrated with a constant Kerr nonlinearity [4].

Here we consider *quadratic nonlinear photonic crystals* (QNPCs) that have a linear grating (periodic dielectric constant) and/or a nonlinear grating (periodic second-order or $\chi^{(2)}$ susceptibility). QNPCs are of interest for all-optical components due to the fast and strong nonlinearity they can provide through the parametric cascading effect [5]. The efficiency of the cascading process depends critically on the phase mismatch between the fundamental and second-harmonic (SH) waves, but two powerful methods exist that use exactly a periodic photonic crystal structure to control the mismatch [6–9]. In one method, a QNPC with a linear Bragg grating is used to bend the dispersion curve near the PBG [7,10]. However, the short period, which is of the order of the optical wavelength, can be inconvenient. The second scheme, quasi-phase-matching (QPM), controls the phase mismatch using a nonlinear grating with a period equal to the comparatively long beat length (typically of the order of microns) [6,9]. QPM is also possible with linear gratings, but this is much less effective [7,8].

One of the spectacular manifestations of nonlinearity is the soliton, a self-localized entity that can propagate unchanged over long distances. Homogeneous $\chi^{(2)}$ materials support solitons in all dimensions [11], and gap solitons exist in QNPCs with a linear Bragg grating [12]. In this paper we focus on the open fundamental problem of whether solitons exist in one-dimensional (1D) QNPCs with *both a linear and a nonlinear QPM grating*. Such a simultaneous linear grating is difficult to avoid when, for example, creating nonlinear QPM gratings in GaAs/AlAs semiconductors through quantum-well disordering [13].

Solitons exist in 1D QNPCs with only a nonlinear QPM grating [14], but a simultaneous linear grating can reduce the effective $\chi^{(2)}$ nonlinearity [7–9]. Thus the global existence of solitons in such QNPCs is nontrivial. We find soliton solutions that are stable under propagation because of cubic nonlinearities induced by the dual QPM gratings. The QNPC even supports stable bright and dark solitons when there is no effective $\chi^{(2)}$ nonlinearity. This is analogous to the existence of solitons in dispersion-managed fibers with no average dispersion [15].

We consider the interaction of a cw beam (carrier frequency ω) with its SH, propagating in a lossless 1D QNPC under conditions for type I second-harmonic generation (SHG). We assume that the modulation of the refractive index is weak [$\Delta n_j(z)/\overline{n_j} \ll 1$, where $n_j(z)=\overline{n_j}+\Delta n_j(z)$ and j refers to the frequency $j\omega$], such that reflective (and radiative) losses can be neglected. Additionally, we consider only gratings for forward-wave QPM, in which case the grating period is much longer than the optical period, far from the Bragg-reflection regime. The evolution of the slowly varying beam envelopes is then described by [6,16]

$$i\frac{\partial w}{\partial z}+\frac{1}{2}\frac{\partial^2 w}{\partial x^2}+\alpha_1(z)w+\chi(z)w^* v e^{i\beta z}=0,$$

$$i\frac{\partial v}{\partial z}+\frac{1}{4}\frac{\partial^2 v}{\partial x^2}+2\alpha_2(z)v+\chi(z)w^2 e^{-i\beta z}=0, \qquad (1)$$

where $w=w(x,z)$ and $v=v(x,z)$ are the envelope functions of the fundamental and SH, respectively. The transverse and propagation coordinates x and z are in units of the input beam width x_0 and the diffraction length $L_d=k_1 x_0^2$, respectively. The parameter $\beta=\Delta k L_d$ is proportional to the mismatch $\Delta k=k_2-2k_1$, $k_j=j\omega\overline{n_j}/c$ being the average wave number. Thus β is positive for normal dispersion and negative for anomalous dispersion. The normalized refractive index grating is given by $\alpha_j(z)=L_d\omega\Delta n_j(z)/c$ and the normalized nonlinear grating by $\chi(z)=L_d\omega d_{\rm eff}(z)/(\overline{n_1}c)$, where $d_{\rm eff}=\chi^{(2)}/2$ is in SI units. The model (1) describes both temporal and spatial solitons [16].

The aim is now to average Eqs. (1) and derive accurate equations for the average field. To do so we focus on first-

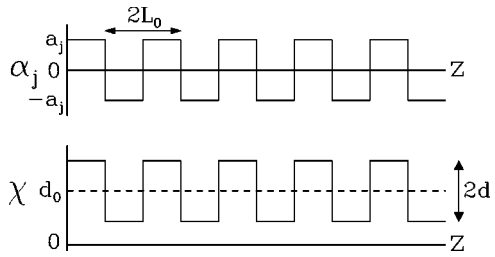

FIG. 1. Normalized linear and quadratic nonlinear gratings, $\alpha_j(z)$ and $\chi(z)$, with period $2L_0=2\pi/|\kappa|$.

order QPM using the conventional square gratings with 50% duty cycle, shown in Fig. 1. We expand the grating functions in a Fourier series,

$$\alpha_j(z)=a_j\sum_n g_n e^{in\kappa z}, \quad \chi(z)=d_0+d\sum_n g_n e^{in\kappa z}, \quad (2)$$

where $g_n=2s/(i\pi n)$ for n odd and $g_n=0$ for n even, with $s=\mathrm{sgn}(\kappa)$. The gratings drive the system and thus we may expand the envelope functions in a Fourier series also,

$$w=\sum_n w_n(z,x)e^{in\kappa z}, \quad v=\sum_n v_n(z,x)e^{i(n\kappa-\tilde{\beta})z}, \quad (3)$$

assuming that the coefficients $w_n(z,x)$ and $v_n(z,x)$ vary slowly in z compared to $\exp(i\kappa z)$. The residual mismatch $\tilde{\beta}=\beta-\kappa$ is ideally zero.

Three physical length scales are in play: the diffraction length L_d, the coherence length L_c, and the grating domain length L_0. In normalized units $L_d=1$, $L_c=\pi/|\beta|$, and $L_0=\pi/|\kappa|$. We assume a typical QPM grating with a domain length that is much shorter than the diffraction length, $L_0\ll 1$. Furthermore, the grating is of good quality, with the domain length being close to the coherence length, $L_0\simeq L_c$, so the residual mismatch is small, $|\tilde{\beta}|\ll|\kappa|$. In this case $|\kappa|\gg 1$ and we can use perturbation theory with the small parameter $\epsilon=1/|\kappa|\ll 1$.

Following the approach of Ref. [14], we insert the Fourier expansions (2) and (3) into the dynamical equations and assume the harmonics $w_{n\neq 0}$ and $v_{n\neq 0}$ to be of order ϵ. To lowest order (ϵ^1), this gives the harmonics

$$w_{n\neq 0}=[a_1 g_n w_0+(dg_{n-1}+d_0\delta_{n,1})w_0^* v_0]/(n\kappa),$$

$$v_{n\neq 0}=[2a_2 g_n v_0+(dg_{n+1}+d_0\delta_{n,-1})w_0^2]/(n\kappa). \quad (4)$$

Using these solutions, we obtain to first order ϵ the averaged equations for the dc components w_0 and v_0,

$$i\frac{\partial w_0}{\partial z}+\frac{1}{2}\frac{\partial^2 w_0}{\partial x^2}+\rho w_0^* v_0+\gamma(|v_0|^2-|w_0|^2)w_0=0,$$

$$i\frac{\partial v_0}{\partial z}+\frac{1}{4}\frac{\partial^2 v_0}{\partial x^2}+\tilde{\beta}v_0+\rho^* w_0^2+2\gamma|w_0|^2 v_0=0. \quad (5)$$

These equations also describe mth order QPM (where $\tilde{\beta}=\beta-m\kappa$ is ideally zero) and any other type of periodic grating, the parameters ρ and γ being simply given as sums over the Fourier coefficients of the grating [14]. Incorporating time or the spatial y coordinate is also straightforward. For the square grating (2), ρ and γ can be explicitly calculated as

$$\rho=i\frac{2d}{s\pi}+i\frac{4d_0(a_1-a_2)}{s\pi\kappa}, \quad \gamma=\frac{d_0^2+d^2(1-8/\pi^2)}{\kappa}. \quad (6)$$

From Eqs. (5) follows the important result that *cubic nonlinearities are induced in QNPCs* by nonlinear QPM gratings. This cubic nonlinearity has the form of self-phase modulation (SPM) and cross-phase modulation, and is a result of non-phase-matched coupling between the wave at the main spatial frequency κ and its higher harmonics. It is thus of a fundamentally different nature than the material Kerr nonlinearity, which is reflected in the fact that the SPM term is absent for the SH.

Apart from sign changes arising from differing definitions of Δk and ρ, the averaged model (5) is similar *in form* to the known model for nonlinear QPM gratings with no dc component ($a_j=d_0=0$), in which bright solitons have properties not predicted by the conventional model with only quadratic terms [14]. The induced cubic nonlinearity also affects the phase modulation of cws, enabling efficient switching [17], and its strength can be increased by modulation of the grating [18].

For the more general QNPCs considered here, the induced cubic nonlinearity depends on both the dc part and the modulation part of the nonlinear grating. It gives either a focusing or a defocusing effect, depending on the relative intensity of the fields and the sign of the phase mismatch β, since $\mathrm{sgn}(\kappa)=\mathrm{sgn}(\beta)$. The defocusing case was not considered in previous studies [14]. The strength of the effective $\chi^{(2)}$ nonlinearity depends on the difference in the linear grating strengths at the fundamental and SH frequencies and on the dc component of the nonlinear grating. We thus recover the well-known effect that the interplay between the linear and nonlinear gratings can increase or decrease the effective $\chi^{(2)}$ nonlinearity, depending on the physical situation [7,8].

The averaged model (5) has stationary, localized soliton solutions of the form $w_0(x,z)=e^{i\lambda z}\tilde{w}(x)/|\rho|$ and $v_0(x,z)=e^{2i\lambda z}\tilde{v}(x)/\rho$, which obey the equations

$$\frac{1}{2}\frac{\partial^2\tilde{w}}{\partial x^2}-\lambda\tilde{w}+\tilde{w}\tilde{v}+\tilde{\gamma}(\tilde{v}^2-\tilde{w}^2)\tilde{w}=0,$$

$$\frac{1}{4}\frac{\partial^2\tilde{v}}{\partial x^2}+(\tilde{\beta}-2\lambda)\tilde{v}+\tilde{w}^2+2\tilde{\gamma}\tilde{w}^2\tilde{v}=0, \quad (7)$$

where $\tilde{\gamma}=\gamma/|\rho|^2$ depends only on κ, a_1-a_2, and d_0/d. The slowly varying approximation gives valid solutions when the soliton period is longer than the grating period, i.e., when the soliton parameter λ is small, $|\lambda|\ll|\kappa|$. Equations (7) cover a much more general situation than in [14], which only con-

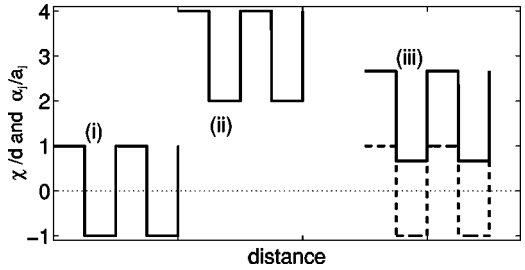

FIG. 2. QNPCs with the same value of $\tilde{\gamma}$. The linear (nonlinear) grating is shown with a dashed (solid) curve.

sidered a nonlinear grating. A given value of the parameter $\tilde{\gamma}$ represents *a range of physical situations with different combinations of linear and nonlinear gratings*. In Fig. 2 we illustrate representative combinations for exact phase matching ($\tilde{\beta}=0$) all of which give the same value of $\tilde{\gamma}$.

The first, simple case (i) is typical for domain inversion in ferroelectric materials, such as $LiNbO_3$. It has only a nonlinear grating with no dc component, $d_0=0$. Case (ii) has a dc component $d_0/d=3$ but no linear grating, corresponding to the nonlinear part of the $LiNbO_3$/H:$LiNbO_3$ structure reported in [19]. Case (iii) is the GaAs/$Ga_{0.8}Al_{0.2}As$ structure reported in [19], which has a nonlinear grating with $d_0/d=5/3$ and a linear grating with $(a_1-a_2)/\beta=-0.07$. So that cases (ii) and (iii) give the same $\tilde{\gamma}$ as in (i), the grating wave number κ is a factor $f=48.5$ and $f=26.6$ larger, respectively [by definition $f=1$ for case (i)]. Physically this corresponds to changing the input beam width x_0, for a constant $\tilde{\beta}=0$.

We have numerically found the bright soliton solutions of Eqs. (7) using a standard relaxation technique. Figure 3 shows soliton properties for normal ($\tilde{\gamma}=0.02$) and anomalous ($\tilde{\gamma}=-0.02$) dispersion, together with the zeroth-order solution ($\tilde{\gamma}=0$). The ratio $R=\tilde{v}^2(0)/\tilde{w}^2(0)$ of peak intensities, shown in Fig. 3(a), confirms that the zeroth-order approximation becomes increasingly inaccurate for large λ. Also, for a given $\tilde{\gamma}$, R approaches the same limiting value as λ increases, regardless of the value of $\tilde{\beta}$. In this limit the SH is stronger than the fundamental for $\tilde{\gamma}>0$ ($R>1$) and much weaker for $\tilde{\gamma}<0$ ($R\simeq 0$). The total power $P=\int_{-\infty}^{\infty}(\tilde{v}^2+\tilde{w}^2)dx$ is shown in Fig. 3(b). For $\beta>0$ this reveals that the

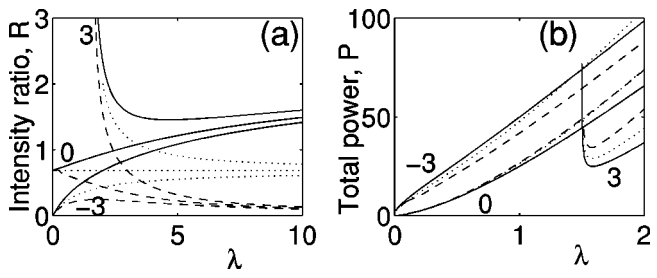

FIG. 3. Soliton properties versus the internal parameter λ for $\tilde{\gamma}=0.02$ (solid), $\tilde{\gamma}=-0.02$ (dashed), and $\tilde{\gamma}=0$ (dotted), and three values of the residual mismatch $\tilde{\beta}$. (a) Ratio of peak intensities $R=\tilde{v}^2(0)/\tilde{w}^2(0)$. (b) Total power P.

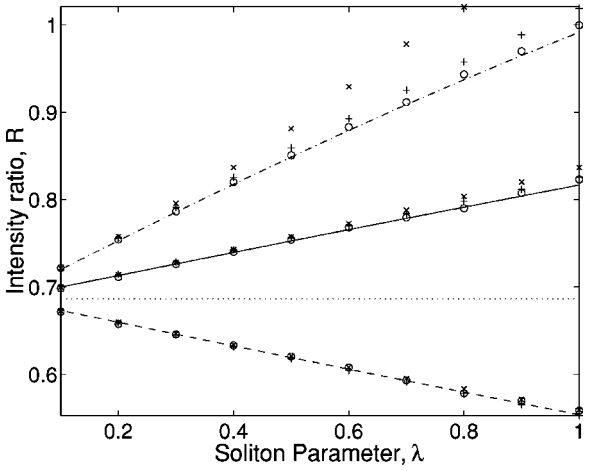

FIG. 4. Ratio of peak intensities $R=\tilde{v}^2(0)/\tilde{w}^2(0)$ versus λ for $\kappa=10f$ (continuous), $\kappa=4f$ (dot-dashed), and $\kappa=-10f$ (dashed), and for the zeroth-order solution (dotted). The averages of the propagating solitons are shown for case (i) by crosses, (ii) by circles, and (iii) by pluses. $\tilde{\beta}=0$.

power threshold for existence decreases for $\tilde{\gamma}>0$ and increases for $\tilde{\gamma}<0$ compared to the zeroth-order value.

We tested the bright soliton solutions of the average model (5) for the three QNPCs of Fig. 2 by mapping them back to the variables w and v, and using them as initial conditions in simulations of the field Eqs. (1). The evolution consists of small, regular oscillations superimposed on the slow average beam. Properties of the propagating solitons were calculated by averaging over an integer number of grating periods and were then compared with the predictions of the average model. Figure 4 displays the ratio of peak intensities versus λ for exact phase matching, $\tilde{\beta}=0$, and reveals that, for both anomalous and normal dispersion, the solutions of the average model are accurate for small λ and large $|\kappa|$, as expected. Even when $|\kappa|=4$ the first-order solutions provide a much better fit than the zeroth-order solutions. Our analysis thus shows that bright solitons exist and propagate stably in QNPCs with many types and combinations of linear and nonlinear QPM gratings.

The competition between linear and nonlinear gratings can drastically alter the relative strength of the $\chi^{(2)}$ nonlinearity. For the $LiNbO_3$ and GaP/AlP structures given in [19] at phase matching ($\kappa=\beta$), the presence of the linear grating changes the effective $\chi^{(2)}$ nonlinearity by a factor of $\mathcal{F}=1+2d_0(a_1-a_2)/(d\kappa)=1.4$ and 0.3, respectively. The linear grating thus adds constructively in the $LiNbO_3$ structure and destructively in GaP/AlP. In fact, modifying the nonlinear grating in the GaP/AlP structure slightly to $\chi_a^{(2)}=40$ pm/V (max) and $\chi_b^{(2)}=19$ pm/V (min) eliminates the effective $\chi^{(2)}$ nonlinearity entirely. This could happen in realistic QNPCs without a violation of the assumption $|\kappa|\gg 1$.

Conventional average models [7–9] would predict that no soliton could exist with no nonlinearity, $\rho=0$. However, in the model (5) the induced cubic nonlinearity predicts that solitons should still exist as solutions of nonlinear Schrödinger equations. In the case when the SH is strong

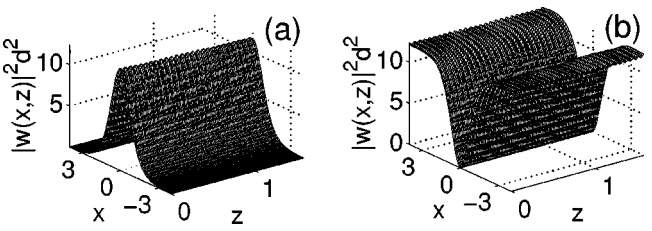

FIG. 5. (a) Bright and (b) dark solitons propagating in QNPCs with no effective $\chi^{(2)}$ nonlinearity. Shown is the scaled intensity of the fundamental for $|\kappa|=100$, $\tilde{\beta}=0$, and (a) $\gamma<0$, $\lambda=1$ and (b) $\gamma>0$, $\lambda=-1$. The SH is zero.

$[v_0/w_0=\sqrt{5}\exp(i(\tilde{\beta}-\lambda/2)z)]$, a family of bright solitons, $w_0=\sqrt{\lambda/(2\gamma)}\,\mathrm{sech}(\sqrt{2\lambda}x)e^{i\lambda z}$, exists for normal dispersion $(\gamma,\lambda>0)$, and a family of dark solitons, $w_0=\sqrt{\lambda/(4\gamma)}\tanh(\sqrt{|\lambda|}x)e^{i\lambda z}$, exists for anomalous dispersion $(\gamma,\lambda<0)$. With no SH, bright solitons, $w_0=\sqrt{2\lambda/|\gamma|}\,\mathrm{sech}(\sqrt{2\lambda}x)e^{i\lambda z}$, exist for anomalous dispersion $(\gamma<0,\lambda>0)$, whereas dark solitons, $w_0=\sqrt{|\lambda|/\gamma}\tanh(\sqrt{|\lambda|}x)e^{i\lambda z}$, exist for normal dispersion $(\gamma>0,\lambda<0)$. We test these solutions also in simulations of the field Eqs. (1).

Figure 5 shows the evolution of a bright and dark soliton with no SH over a distance of 25 grating periods. Reflective losses, if included, would cause a decrease in amplitude of approximately 5% because of the relatively large index change for this case. The SH displays small, regular oscillations around the mean value zero, corresponding to the oscillations of the fundamental seen in Fig. 5. The simulations thus confirm that bright and dark solitons can indeed propagate in a stable manner in QNPCs with no effective $\chi^{(2)}$ nonlinearity.

In summary, we have shown that bright solitons exist and propagate in a stable manner in 1D QNPCs with many types and combinations of linear and nonlinear QPM gratings. By deriving first-order averaged equations, we have shown that such QNPCs have an induced cubic nonlinearity, and we have numerically found previously unknown families of bright solitons. Even with no effective quadratic nonlinearity, the QNPCs support both bright and dark solitons due to the induced cubic nonlinearity. We have found analytical expressions for these solitons and shown that they also propagate in a stable manner. Dark solitons are always unstable in homogeneous $\chi^{(2)}$ media in settings for type I SHG, due to modulational instability of the background plane waves [20]. Because we have allowed for defocusing induced cubic nonlinearity, our results show a dark soliton that appears to be stable under propagation, with the stabilizing mechanism necessarily originating from the photonic crystal structure of the QNPC. Such stabilizing mechanisms are of considerable experimental interest [21]. A study of dark solitons in the general case is in progress [22].

The project is supported by the Danish Technical Research Council through Grant No. 26-00-0355.

[1] *Photonic Band Gap Materials*, Vol. 315 of *NATO Advanced Studies Institute, Series E: Applied Sciences*, edited by C. M. Soukoulis (Kluwer Academic, Dordrecht, 1996).
[2] S.W. Leonard *et al.*, Phys. Rev. B **61**, R2389 (2000).
[3] K. Busch and S. John, Phys. Rev. Lett. **83**, 967 (1999).
[4] S. Larochelle *et al.*, Electron. Lett. **26**, 1459 (1990).
[5] For a review, see G.I. Stegeman, D.J. Hagan, and L. Torner, Opt. Quantum Electron. **28**, 1691 (1996).
[6] J.A. Armstrong *et al.*, Phys. Rev. **127**, 1918 (1962).
[7] C.L. Tang and P.P. Bey, IEEE J. Quantum Electron. **9**, 9 (1973).
[8] B. Jaskorzynska, G. Arvidsson, and F. Laurell, *Integrated Optical Circuit Engineering* (SPIE, Bellingham, WA, 1986), Vol. III, p. 221.
[9] M.M. Fejer *et al.*, IEEE J. Quantum Electron. **28**, 2631 (1992); C.Q. Xu, H. Okayama, and M. Kawahara, *ibid.* **31**, 981 (1995).
[10] N. Bloembergen and A.J. Sievers, Appl. Phys. Lett. **17**, 483 (1970).
[11] For a review, see L. Torner, in *Beam Shaping and Control with Nonlinear Optics*, edited by F. Kajzer and R. Reinisch (Plenum, New York, 1998).
[12] Y.S. Kivshar, Phys. Rev. E **51**, 1613 (1995); for a recent overview see A. Arraf and C.M. de Sterke, *ibid.* **58**, 7951 (1998).
[13] A. Saher Helmy *et al.*, Opt. Lett. **25**, 1370 (2000).
[14] C.B. Clausen, O. Bang, and Y.S. Kivshar, Phys. Rev. Lett. **78**, 4749 (1997).
[15] J.H.B. Nijhof *et al.*, Electron. Lett. **33**, 1726 (1997); S.K. Turitsyn and E.G. Shapiro, Opt. Lett. **23**, 682 (1998).
[16] C.R. Menyuk, R. Schiek, and L. Torner, J. Opt. Soc. Am. B **11**, 2434 (1994); O. Bang, *ibid.* **14**, 51 (1997).
[17] A. Kobyakov *et al.*, Opt. Lett. **23**, 506 (1998); O. Bang, T.W. Graversen, and J.F. Corney, *ibid.* **26**, 1007 (2001).
[18] O. Bang *et al.*, Opt. Lett. **24**, 1413 (1999).
[19] D.V. Petrov, Opt. Commun. **131**, 102 (1996).
[20] S. Trillo and P. Ferro, Opt. Lett. **20**, 438 (1995); A.V. Buryak and Y.S. Kivshar, *ibid.* **20**, 834 (1995).
[21] P. Di Trapani *et al.*, Phys. Rev. Lett. **84**, 3843 (2000).
[22] J.F. Corney and O. Bang, Phys. Rev. Lett. (to be published).